International Geotechnical Symposium on Theory and Practice of Earth Reinforcement / Fukuoka Japan / 5-7 October 1988

Prediction of bearing capacity in level sandy ground reinforced with strip reinforcement

Ching-Chuan Huang
University of Tokyo, Tokyo, Japan
Fumio Tatsuoka
Institute of Industrial Science, University of Tokyo, Japan

ABSTRACT: The bearing capacity of footing placed on level ground can be increased by placing horizontal layers of tensile reinforcing strips beneath the footing. A series of model tests were performed in order to investigate the reinforcing mechanism and develop a method for calculating the increase in the bearing capacity by reinforcing.

1 INTRODUCTION

The failure mechanism of level ground reinforced with long strips was assumed by Binquet and Lee(1975 a,b) as illustrated in Fig. 1 ; the active zone including a part of the strips was anchored by the remaining parts of strips located outside the active zone. It indicates that only the strips extending beyond the footing width can increase the bearing capacity.

The failure mechanism of reinforced level sandy ground loaded by a strip footing observed in the present study was very different from that mentioned above; at the peak footing load, shear bands were developed only in a limited area beneath the footing, with small strains outside the active zone. Further, by restraining possible strains in soil in the zone beneath the footing by means of short strips with the same length as the footing width, the bearing capacity was inceased remarkedly. Based on these results, a new stability analysis method by using limit equilibrium method was developed.

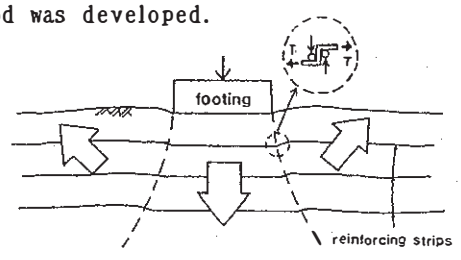

Fig. 1 Failure mechanism assumed by Binquet and Lee 1975 a, b.

2 MODEL TEST ARRANGEMENT

Model grounds were constructed by pluviating air-dried Toyoura sand through air at a controlled fall height in a sand box as shown in Fig. 2. By this method, homogeneous models having very similar dry densities γ_d were produced. Toyoura sand has a mean diameter of 0.16mm, a coefficiet of uniformity of 1.46 and a sub-angular to angular particle shape. The strength and deformation properties have been thoroughly studied by Tatsuoka et al. (1986).

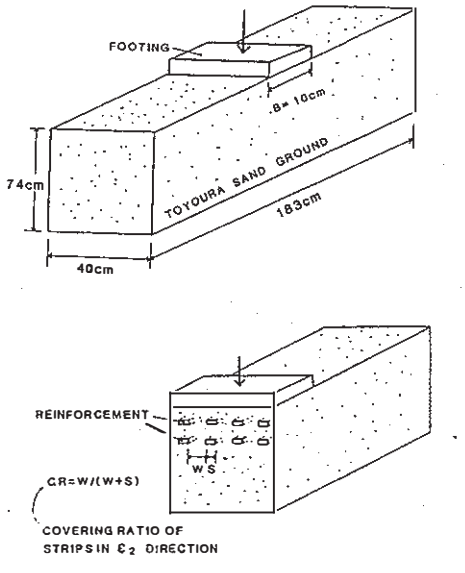

Fig. 2 Model test arrangement.

A rigid, rough, strip footing, which was 10 cm wide, guided against tilting was loaded at a constant axial displacement of 0.1mm-0.2mm/min. The side walls consisted of 3cm-thick transparent acryl plates with steel stiffeners outside. In order to reduce the effect of side-wall friction, the inside surface of each acryl plate was lubricated by means of a 0.05mm thick silicone grease layer and a 0.2mm thick membrane. Further, only the load at the central third of the footing was measured.

On the outside surface of membrane, 1cm-square grids were drawn. Strain fields on the lateral plane of model were constructed from the displacements of the nodes read to an accuracy of about 0.01mm using the pictures, which were taken occasionally during each test. From these pictures, shear bands also were identified.

Reinforcing strips, 0.5mm thick and 3mm wide, were made of phosphor bronze. Their surfaces were made rough by glueing model sand particles. The tensile forces were measured by means of strain gages attached to the strips.

The following four groups of tests were performed(see Fig.3):

Group-a: to study the reinforcing effect of short strips having the same length as the footing width B(=10cm). Additionally, three tests in which footing was placed on unreinforced ground were performed as reference tests.

Group-b: to study the effect of the length of reinforcement.

Group-c: to study the effect of the number of reinforcement layers.

Group-d: to study the effect of density of reinforcing strips(the effect of covering ratio CR as explained in Fig.2) .

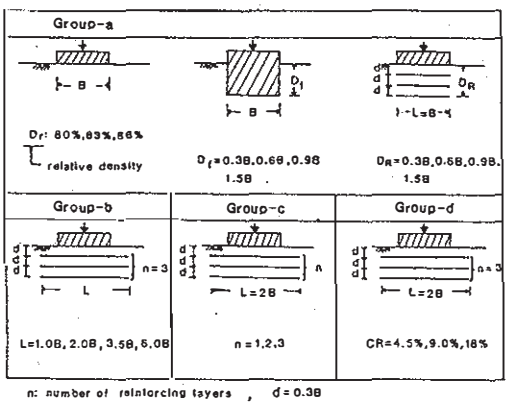

Fig.3 Groups of test in present study.

3. FAILURE MECHANISM OF UNREINFORCED GROUND LOADED BY SURFACE OR DEEP FOOTING

The relationships between the normalized footing pressure N and s/B (footing settlement/ footing width)for Group-a are shown in Fig.4. Here $N=2*q/(\gamma_d*B)$, where q is the average footing pressure. It may be seen that the strength of reinforced ground increases in a very similar way to that by deeping the footing to the depth which is equivalent to that of the bottom layer of reinforcement(D_R).

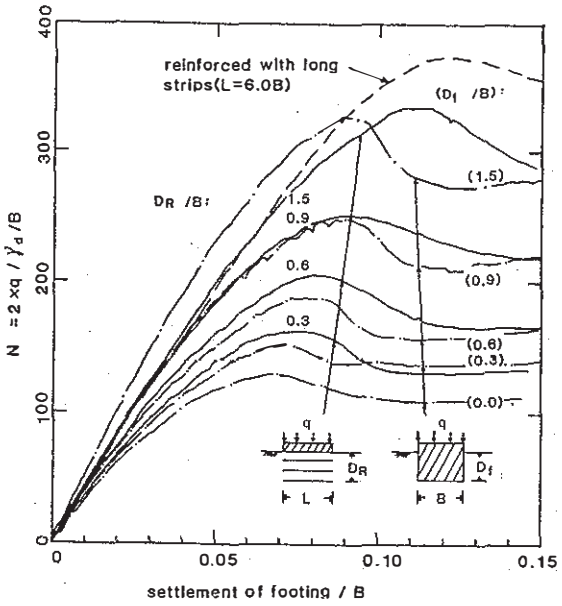

Fig.4 Results of Group-a .

Fig.5 shows the strain field in the unreinforced ground near the peak footing load. The lengths and directions of the two crossed segments represent the magnitudes and directions of the major and minor (extensional) principal strains developed for s/B=0.0 -> 0.07. The triangle beneath the footing is the wedge observed. Intensely strained bands may be seen only along the wedge(or active zone). Outside the active zone, only very limited strains can be seen.

This result suggests that the failure in such an unreinforced sand ground is rather progressive and the axial compressive strength of the active zone beneath the footing controls the bearing capacity of the ground.

Thus, it was assumed that the bearing capacity q_u for unreinforced ground loaded by a surface footing can be expressed by:

$$q_u = q_1 + q_2 \qquad (1)$$

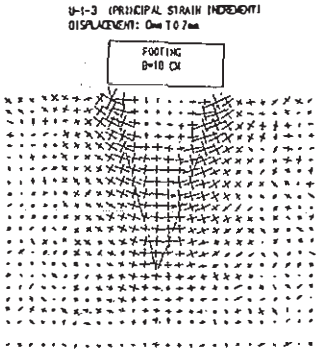

Fig. 5 Strain field for unreinforced ground at peak loading.

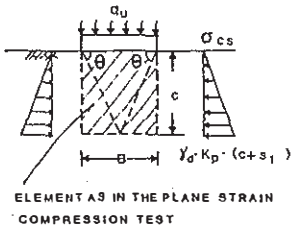

Fig. 6 Schematic failure model for unreinforced ground.

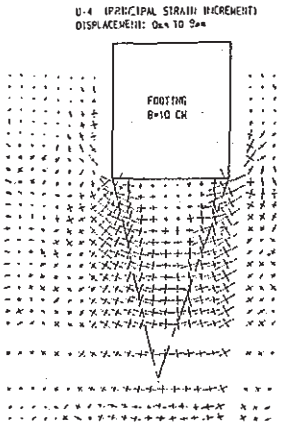

Fig. 7 Strain field for deep footing at peak loading.

q_1: the compressive strength of a block including the active zone, which is considered to behave like an element in the plane strain compression (PSC) test (Fig. 6), and is assumed to be expressed by :

$$q_1 = K_p * \sigma_{cs} \quad (2)$$

$K_p = \tan^2(45° + \phi/2)$

ϕ = the internal friction angle of sand in the corresponding PSC test

$$\sigma_{cs} = \gamma_d * K_p * (c+s_1)/2 \quad (3)$$

γ_d = dry density of sand

c, s_1 = the length of block and the settlement of footing at failure (see Fig. 6).

q_2 is the bearing capacity component induced by the following factor, such as the friction at the lateral faces of the block element which do not exist in a PSC test.

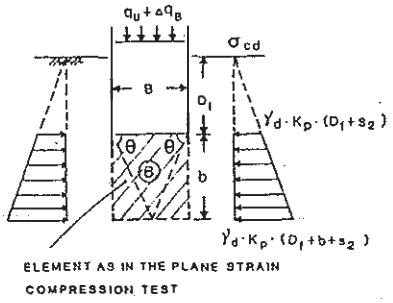

Fig. 8 Schematic failure model for deep footing.

Also in the unreinforced ground beneath a deep footing with a footing depth $D_f = 0.9B$, a strain field (see Fig. 7) similar to the one seen in Fig. 5 was observed. Thus, a similar equation to Eq. 1 was assumed for the bearing capacity q_B for a deep footing:

$$q_B = q_3 + q_4 \quad (4)$$

q_3 = the compressive strength of a block (denoted by B in Fig. 8) beneath the deep footing, which is considered to behave like an element in a PSC test;

$$q_3 = K_p * \sigma_{cd} \quad (5)$$

$$\sigma_{cd} = \gamma_d * (2D_f + b + 2s_2)/2 \quad (6)$$

D_f, b, s_2: the depth of footing, the length of block and the settlement of footing at failure (see Fig. 8).

4 FAILURE MECHANISM OF REINFORCED GROUND LOADED BY A SURFACE FOOTING

Fig. 9 shows the strain field for the ground densely reinforced with short strips of L=B (Group-a) with a depth of the reinforced zone of $D_R = 0.9B$. It may be seen that this strain field is very similar to that for a deep footing with the same depth $D_f = 0.9B$ shown in Fig. 7. It may also be seen from Fig. 4 that each ground reinforced with short strips of L=B behave very similarly to the corresponding deep footing of $D_f = D_R$. This trend exists especially in the case of $D_R \leqq 0.9B$, and such a reinforcing effect may be called "the deep footing effect".

Fig. 10 shows the strain field for the ground densely reinforced with long strips of L=6B (Group-b) with a depth of the reinforced zone D_R equal to 0.9B. It may be seen that this strain field is similar to that for the case of short strips shown in Fig. 9 in the sense that the strain in the reinforced zone beneath the footing is effectively restrained and below the reinforced zone an intensely strained zone is formed.

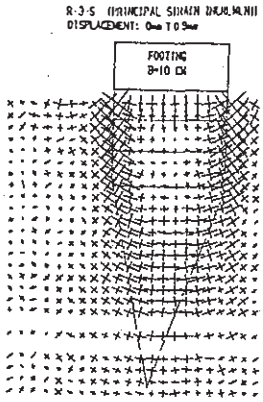

Fig.9 Strain field for the ground densely reinforced with short strips.

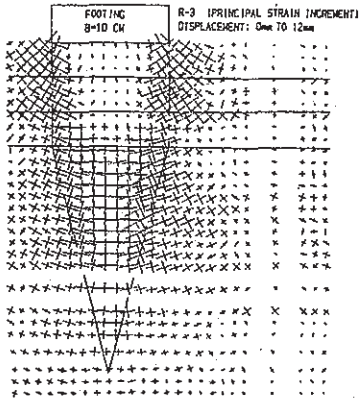

Fig.10 Strain field for the ground densely reinforced with long strips.

As seen from Fig.4, only small strength increase can be obtained by increasing the length of reinforcing strips from 1.0B to 6.0B. This result implies that the major part of the increase in the bearing capacity by reinforcing is due to "the deep footing effect", and a further increase is due to the side wall friction on the restrained zone.

The patterns of shear band observed at the peak footing load in all reinforced grounds can be claassified into the following two types, depending on the density of strips.

For densely reinforcing conditions(for either short or long strips), shear bands starting from the footing edges extends straightly downward approximately to the depth D_R, then form a wedge beneath the reinforced zone. This failure mode is called Failure mode-1 . In this case, the bearing capaciy of reinforced ground is controlled by the strength of the zone including the wedge denoted by B (see Fig. 11 a).

For lightly reinforcing conditions, the shear bands starting from the footing edges form a wedge within the reinforced zone, but the apex of the wedge is deeper than that for the unreinforced ground(see Fig. 11 b).

This failure mode is called Failure mode-2 In this case, the bearing capacity of the reinforced ground is conrolled by the strength of the block A immediately beneath the footing.

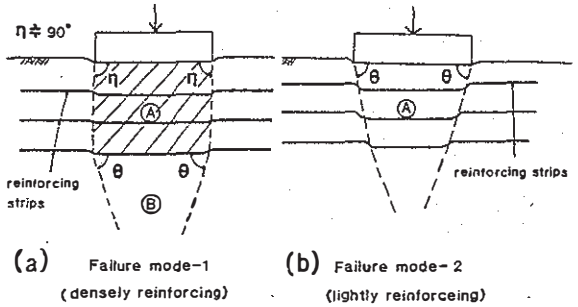

Fig. 11(a), (b) Failure modes observed in the present study.

5 ANALYSIS OF REINFORCING EFFECT

The observed angles θ of shear bands defined from the horizontal line were slightly scattered as $\theta=45°+\phi/2+(3°\sim7°)$ (ϕ is the angle of internal friction in the condition of σ_1-direction vertical to the bedding plane, refer to Tatsuoka et al.1986. In the present study, ϕ is in the range of 48.8°—50.2° .Since the effect of the small variation of θ (3°～7°) on the results of analysis was found negligible, in the following, $\theta=45°+\phi/2$ was assumed.

5.1 Increase in bearing capacity for Failure mode-1(deep footing effect)

From Eqs.(1) and (4), the increace in the bearing capacity due to deeping a rigid footing is

$$\Delta q_B=q_B-q_u=q_3-q_1+(q_4-q_2) \quad (7)$$

By assuming that q_2-q_4 is relatively small and can be neglected, we obtain:

$$\Delta q_B=q_3-q_1 \quad (8)$$

For Failure mode-1, the increace in the bearing capacity due to reinforcing also is obtained by Eq. 8.

The results of the analysis are shown in Fig. 12, in which,

$$BCR_B(\text{predicted})=(q_u+\Delta q_B)/q_u. \quad (9)$$

q_u is obtained from the reference test in Group-a for the same sand density as that for Δq_B by using the method of interpolation. In the following, the same method was used for obtaining q_u. In Fig. 12 the measured bearing capacities of deep footing in unreinforced grounds $q_u(D_f>0)$ are

expressed by:

$BCR(\text{measured}) = q_u(D_f>0)/q_u$ (10)

It may be seen from Fig. 12 that the values predicted by Eq. (8) agree fairly well with the measured values both for the deep footings and the reinforced grounds. Thus, it is concluded that the effect of densely reinforcing with short strips is very similar to that by deeping the footing to the depth of the bottom layer of reinforcement.

It is assumed that for the case of long strips ($L>B$), the tensile forces in the reinforcements outside the block A increase the normal forces on the side wall of Element A, and hence increase the upward side wall friction ΔS (see Fig. 13). Thus, the bearing capacity increase for a ground reinforced with strips of $L>B$, Δq_c, is expressed by:

$$\Delta q_c = \Delta q_B + \Delta S \quad (9)$$

Δq_B : from Eq. (8)

$$\Delta S = 2*\{\sum_{i=1}^{n} T_{e.i}*\tan\phi*N_i\}/B \quad (10)$$

n : the number of layers

N_i : the number of strips per unit length in the σ_2 direction at layer i.

B : the width of footing

$T_{e.i}$: the tensile force in strip i at the side faces of Element A. It is zero for L=B.

In the following analysis, the tensile fores measured at peak footing load are used In the case of L=B, ΔS is equal to 0, thus $BCR_B = BCR_c$.

Similarly, The predicted Δq_c can be expressed by:

$BCR_c(\text{predicted}) = (q_u + \Delta q_c)/q_u$

and the measured bearing capacity for reinforced grond is expressed by:

$BCR(\text{measured}) = q_u(\text{reinforced})/q_u$

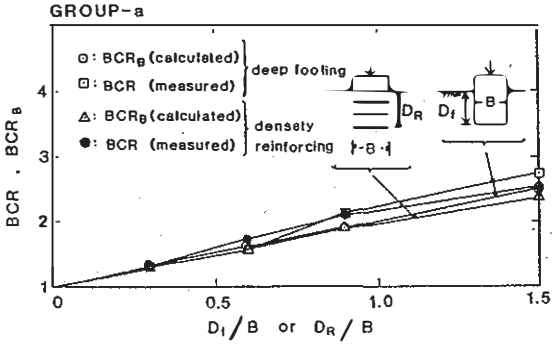

Fig. 12 The results of Group-a.

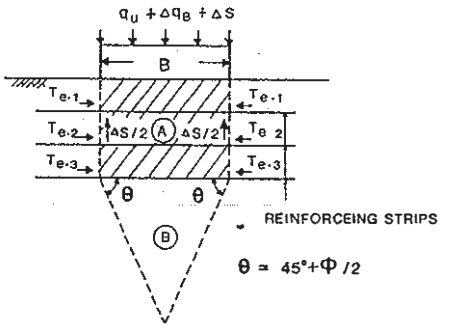

Fig. 13 Schematic model showing the increase in side wall friction.

5.2 Increase in bearing capacity for Failure mode-2

It is assumed that the increase in the compressive strength of Element A (Δq_A) is due to the increase in the lateral confinement induced by tensile forces in the strips, and is expressed by: (see Fig. 14),

$$\Delta q_A = K_p*\sigma_t \quad (11)$$

$$\sigma_t = \{\sum_{i=1}^{n} (T_{av.i}*N_i)\}/D_R \quad (12)$$

N_i : the number of strips per unit length in σ_2 direction at layer i

$T_{av.i}$: averaged tensile force at layer i ($= (T_{max.i}+T_{e.i})/2$) in Block A

$T_{max.i}$ and $T_{e.i}$ are the maximum value of tensile force at the center and at the side of Elenment A in strip i. $T_{e.i}$ is zero for L=B.

Again, the effect of reinforcing for Failure mode-2 can be expressed by:

$BCR_A(\text{predicted}) = (q_u + \Delta q_A)/q_u$

Base on this method, BCR_A and BCR_c for each test were calculated and the smaller one was used for evaluating the effect of reinforcing. It may be seen from Figs. 15, 16, and 17 that the prediction is satisfactory.

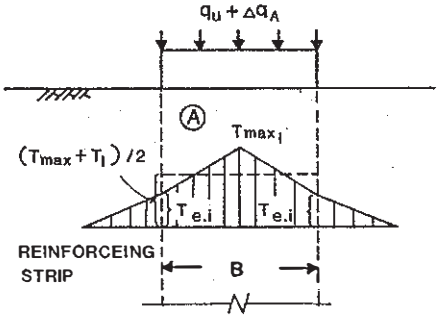

Fig. 14 Schematic model showing the strength increase in reinforced zone A.

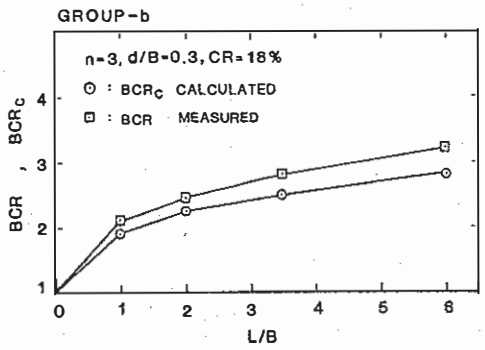

Fig. 15 The results of Group-b.

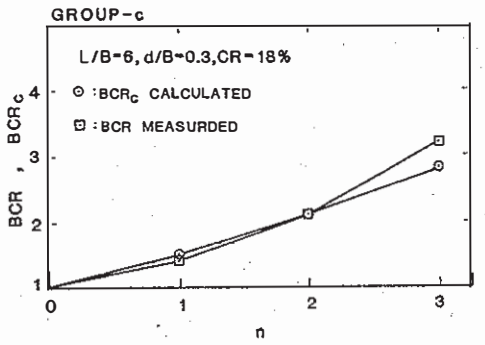

Fig. 16 The results of Group-c,

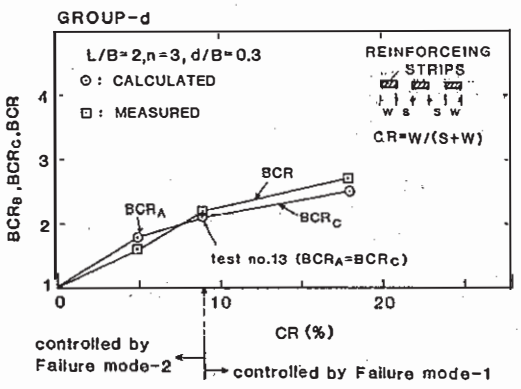

Fig. 17 The results of Group-d.

Theoretically, there exists an optimumn condition for designing when $BCR_A=BCR_C$. In the present study, Test No. 13 ($L/B=2$, $D_R/B=0.9$ $CR=9\%$, see Fig. 17) was found to be the optimum one.

6 CONCLUSION

The failure mechanism in a level ground reinforced with horizontal strips and the analysis of reinforcing effect on the bearing capacity have been presented. In practical conditions, the prediction of tensile forces in reinforcements is essential. An empirical method based on these tests has been developed and will be presented elsewhere in the future.

ACKNOWLEDGEMENT

This paper is a part of Master of Engineering thesis presented by the first author Appreciation is given to Japanese Rotary Yoneyama Foundation which offered a scholorship to the first author from April, 1986 to September, 1987.

REFFERENCES

1) J. Binquet and K. L Lee, 1975a. "Bearing capacity tests on reinforced slabs". Journal of Geotechnical Engineering Devision, ASCE, vol. 101, No. GT12, pp. 1241-1255

2) J. Binquet and K. L. Lee 1975b. "Bearing capacity tests on reinforced slabs". Journal of Geotechnical Engineering Devision, ASCE, vol. 101, No. GT12, pp. 1257-1276

3) Vito A. Guido, Dong K. Chang, and Michael A. Sweeney. "Comparison of geogrid and geotextile reinforced slabs". Canada Geotechnical Journal, vol. 23, No. 4, November 1986, pp. 435-440

4) Ching-Chuan Huang and Fumio Tatsuoka. "Deep-footing effect in bearing capacity of sand reinforced with tensile reinforcement". The 22nd Japan National Conference on Soil mechanics and foundation engineering, June, 1987

5) Kazuo Tani and Fumio Tatsuoka. "Effect of pressure level and model size on bearing capacity of model strip footing on sand". The 22nd Japan National Conference on Soil Mechanics and Foundation Engineering, June, 1987

6) Fumio Tatsuoka, Makoto Sakamoto, Taizo Kawamura and Shinji Fukushima . "Strength and deformation chacteristics of sand in plane strain compression at extremely low pressures". JSSMFE Soils and Foundations, Vol. 26, No. 1, pp. 65-84, March, 1986.